New Insights in Frustrated Lewis Pair Chemistry with Azides

Boom, Devin H. A.

2019-10-17

Boom , D H A , Jupp , A R , Nieger , M , Ehlers , A W & Slootweg , J C 2019 , ' New Insights in Frustrated Lewis Pair Chemistry with Azides ' , Chemistry: A European Journal , vol. 25 , no. 58 , pp. 13299-13308 . https://doi.org/10.1002/chem.201902710

http://hdl.handle.net/10138/307219
https://doi.org/10.1002/chem.201902710

ChemPubSoc Europe
DOI: 10.1002/chem.201902710
CHEMISTRY A European Journal Full Paper

Frustrated Lewis Pairs | *Hot Paper* |

New Insights in Frustrated Lewis Pair Chemistry with Azides

Devin H. A. Boom,[a] Andrew R. Jupp,[a] Martin Nieger,[b] Andreas W. Ehlers,[a, c] and J. Chris Slootweg*[a]

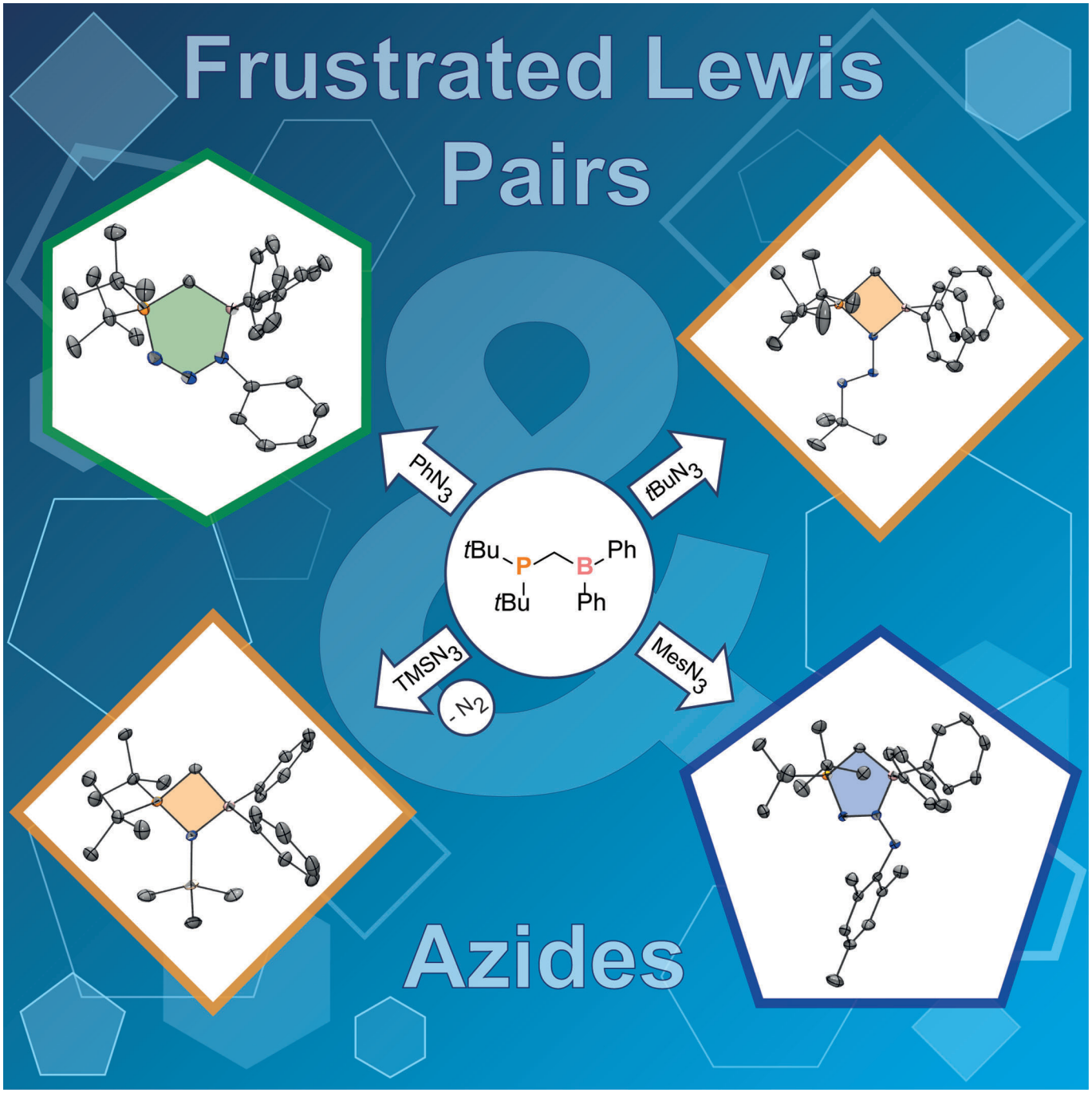

Abstract: The geminal frustrated Lewis pair (FLP) tBu$_2$PCH$_2$BPh$_2$ (**1**) reacts with phenyl-, mesityl-, and *tert*-butyl azide affording, respectively, six, five, and four-membered rings as isolable products. DFT calculations revealed that the formation of all products proceeds via the six-membered ring structure, which is thermally stable with an N-phenyl group, but rearranges when sterically more encumbered Mes–N$_3$ and tBu–N$_3$ are used. The reaction of **1** with Me$_3$Si–N$_3$ is believed to follow the same course, yet subsequent N$_2$ elimination occurs to afford a four-membered heterocycle (**5**), which can be considered as a formal FLP-trimethylsilylnitrene adduct. Compound **5** reacts with hydrochloric acid or tetramethylammonium fluoride and showed frustrated Lewis pair reactivity towards phenylisocyanate.

Introduction

During the past two decades a vast amount of research has been conducted on small-molecule activation utilizing main-group species as viable alternatives to the well-established transition-metal complexes. For example, cyclic (alkyl)(amino)-carbenes (CAACs) can cleave the strong covalent H–H, N–H, P–H, B–C, and B–H bonds,[1–3] and can capture CO and catecholborane.[4,5] Organic azides are common organic molecules and are key building blocks in, for example, the Staudinger reaction, which is the reaction of a phosphine with an azide to form a phosphazene after elimination of dinitrogen.[6] Interestingly, the reaction between N-heterocyclic carbenes (NHCs) and azides offers the opportunity to trap reaction intermediates by an "interrupted Staudinger" reaction[7,8] forming the stabilized triazene moiety **A** (Figure 1)[9,10] that can be functionalized and gives access to highly colored donor–acceptor materials (**B**), which may find new applications in nonlinear optics.[11] The analogous reaction with TMS–N$_3$ (TMS: SiMe$_3$) leads to the facile elimination of dinitrogen and formation of the imidazolidin-2-imine derivative **C**, which can be viewed as a NHC–nitrene adduct. Subsequent cleavage of the TMS group affords the interesting anionic imidazolin-2-iminato ligands, which can coordinate to almost any metal and be utilized in homogeneous catalysis.[12]

Related is the reactivity of frustrated Lewis pairs (FLPs)[13] towards organic azides, but in this case multiple Staudinger intermediates have been isolated. Phosphorus/boron-based FLPs have been shown to add to the α-nitrogen of the azide forming coordination mode **D** (Figure 1)[14] and, in one case, it was found that upon irradiation this species rearranges to α,β-nitrogen adduct **E**.[15] The α,γ-nitrogen coordination mode **F** was found by treating a geminal FLP with mesityl azide.[16,17] In analogy to the reactivity of NHCs (**C**; Figure 1), dinitrogen elimination occurs when TMS azide was reacted with a P/Al-based FLP affording heterocycle **G**,[18] yet in this case no follow-up chemistry has been investigated.

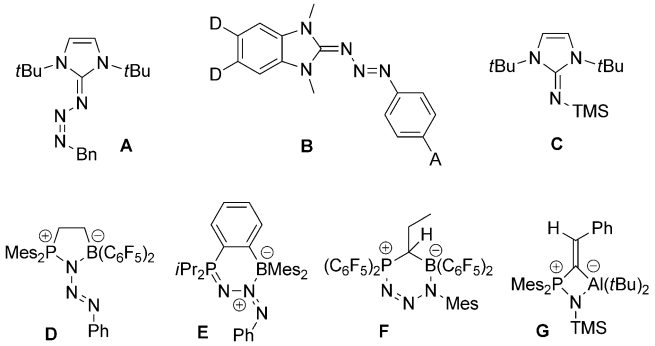

Figure 1. Examples of NHC adducts with azides (top) and FLP adducts with azides (bottom) (EDG = electron-donating group, EWG = electron-withdrawing group).

Given the diverse reactivity of frustrated Lewis pairs with organic azides, we were keen to unravel the mechanistic details of this chemistry as well as to elucidate if all three coordination modes (**D**, **E**, **F**) are interconnected on the potential energy surface. We discovered that by using the geminal phosphorus/boron-based FLP tBu$_2$PCH$_2$BPh$_2$ (**1**)[19] and differently substituted azides all coordination modes can be obtained by formation of the corresponding four, five, and six-membered heterocycles (Scheme 1). In addition, we were keen to investigate the reaction of **1** with Me$_3$Si–N$_3$ and explored the reactivity of the resulting four-membered ring **5**.

Results and Discussion

Treatment of tBu$_2$PCH$_2$BPh$_2$ (**1**) with 1 equiv of Ph–N$_3$ in THF at −10 °C and subsequent warming to room temperature resulted in the immediate conversion to $\mathbf{2_{Ph}}$, which after workup was isolated as a yellow powder in 98% yield ($\delta(^{31}P\{^1H\}) = 31.8$; $\delta(^{11}B\{^1H\}) = -6.8$ ppm; Scheme 1).[20] The molecular structure of $\mathbf{2_{Ph}}$, determined by a single-crystal X-ray diffraction analysis, established unequivocally the formation of a six-membered heterocycle (Figure 2, top left) with P1–N1 (1.687(2) [1.686(2)] Å)

[a] *Dr. D. H. A. Boom, Dr. A. R. Jupp, Dr. A. W. Ehlers, Prof. Dr. J. C. Slootweg*
Van't Hoff Institute for Molecular Sciences, University of Amsterdam,
Science Park 904, 1090 GD Amsterdam (The Netherlands)
E-mail: j.c.slootweg@uva.nl

[b] *Dr. M. Nieger*
Department of Chemistry, University of Helsinki
A. I. Virtasen aukio 1, PO Box 55, 00014 Helsinki, (Finland)

[c] *Dr. A. W. Ehlers*
Department of Chemistry, Science Faculty, University of Johannesburg
PO Box 254, Auckland Park, Johannesburg, (South Africa)

Supporting information and the ORCID identification number(s) for the author(s) of this article can be found under: https://doi.org/10.1002/chem.201902710.

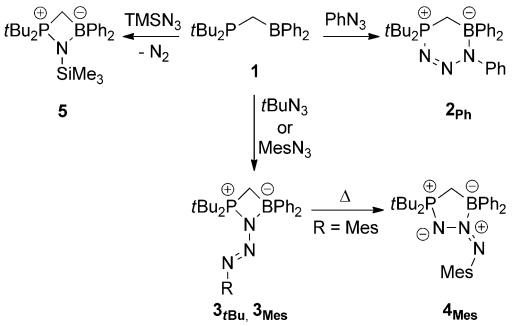

Scheme 1. Reactivity of FLP **1** with phenyl azide ($\mathbf{2}_{Ph}$), *tert*-butyl azide ($\mathbf{3}_{tBu}$), and mesityl azide ($\mathbf{3}_{Mes}$, $\mathbf{4}_{Mes}$) and trimethylsilyl azide (**5**).

and B1–N3 (1.597(3) [1.603(3)] Å) bonds (the numbers in brackets refer to the bond metrics of a second crystallographically independent molecule in the asymmetric unit). Interestingly, $\mathbf{2}_{Ph}$ displays much more localized N–N bonds (N1–N2: 1.290(3) [1.291(3)], N2–N3: 1.323(3) [1.329(3)] Å) compared with **F** (N1–N2: 1.304(3), N2–N3: 1.306(3) Å; Figure 1),[16] which is likely due to the more electron-rich phosphorus center in $\mathbf{2}_{Ph}$.

We wanted to explore the mechanism for the formation of $\mathbf{2}_{Ph}$, and considered two options that differ according to the initial interaction of the azide with the FLP. DFT calculations at the ωB97X-D/6-31G* level of theory showed that the nucleophilic attack of the phosphine to the azide ($\mathbf{TS3}_{Ph}$ $\Delta E^{\ddagger} =$ 9.6 kcal mol^{-1}), which is the first step in the Staudinger reaction[21] is disfavored, and instead nucleophilic attack of the azide to the boron moiety of the FLP is preferred, which leads to $\mathbf{INT1}_{Ph}$ ($\Delta E = 5.2$, $\Delta E^{\ddagger} = 8.0$ kcal mol^{-1}) by formation of a boron-γ-nitrogen bond (Scheme 2). Note that this reaction path is well documented for the related transition metal chemistry with azides,[22,23] yet poorly described for main-group systems.[24] Subsequent ring closure of this Lewis adduct $\mathbf{INT1}_{Ph}$ via $\mathbf{TS2}_{Ph}$ affords the product $\mathbf{2}_{Ph}$ ($\Delta E = -37.2$, $\Delta E^{\ddagger} =$ 3.12 kcal mol^{-1}).

Next, we treated FLP **1** with *t*Bu–N_3 and Mes–N_3 and found that in these cases the reaction rate is significantly slower.

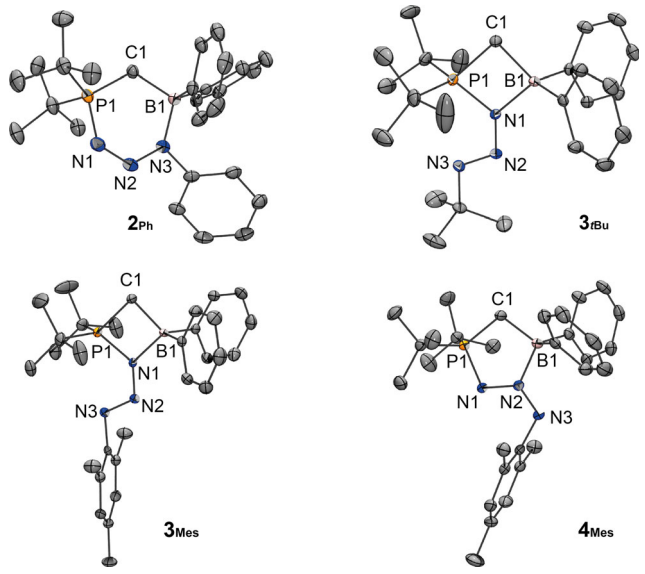

Figure 2. Molecular structures of $\mathbf{2}_{Ph}$, $\mathbf{3}_{tBu}$, $\mathbf{3}_{Mes}$, and $\mathbf{4}_{Mes}$ (ellipsoids at 50% probability, hydrogen atoms and for $\mathbf{2}_{Ph}$ and $\mathbf{4}_{Mes}$ second crystallographic independent molecules omitted for clarity). Selected bond lengths [Å] and angles [°] for $\mathbf{2}_{Ph}$ (structural parameter for the second crystallographic independent molecule in brackets): P1–N1 1.687(2) [1.686(2)], N1–N2 1.290(3) [1.291(3)], N2–N3 1.323(3) [1.329(3)], N3–B1 1.597(3) [1.603(3)]. $\mathbf{3}_{tBu}$: P1–N1 1.6675(12), N1–N2 1.3573(16), N2–N3 1.2502(17), N1–B1 1.6066(19); P1-N1-N2-N3 −1.66(19). $\mathbf{3}_{Mes}$: P1–N1 1.6838(19), N1–N2 1.342(3), N2–N3 1.259(3), N1–B1 1.613(3); P1-N1-N2-N3 0.000(1). $\mathbf{4}_{Mes}$: P1–N1 1.6592(13) [1.6557(13)], N1–N2 1.3364(17) [1.3397(17)], 1.2733(17) [1.2695)], N2–B1 1.668(2) [1.655(2)]; P1-N1-N2-N3 −176.26(11) [175.08(11)].

After addition of 1 equiv of *t*Bu–N_3 or Mes–N_3 to a solution of **1** in THF at 0 °C, at least one hour stirring at room temperature was required for full conversion to product $\mathbf{3}_{tBu}$ or $\mathbf{3}_{Mes}$, respectively ($\mathbf{3}_{tBu}$: $\delta(^{31}P\{^1H\}) = 98.1$; $\delta(^{11}B\{^1H\}) = 3.8$, $\mathbf{3}_{Mes}$: $\delta(^{31}P\{^1H\}) =$ 95.5; $\delta(^{11}B\{^1H\}) = 2.8$ ppm; Scheme 1).[25] The molecular structures of $\mathbf{3}_{tBu}$ and $\mathbf{3}_{Mes}$, determined by single-crystal X-ray diffraction analyses, revealed in both cases the formation of a four-membered heterocycle in which both the donor and acceptor site of FLP **1** are attached to the α-nitrogen of the cor-

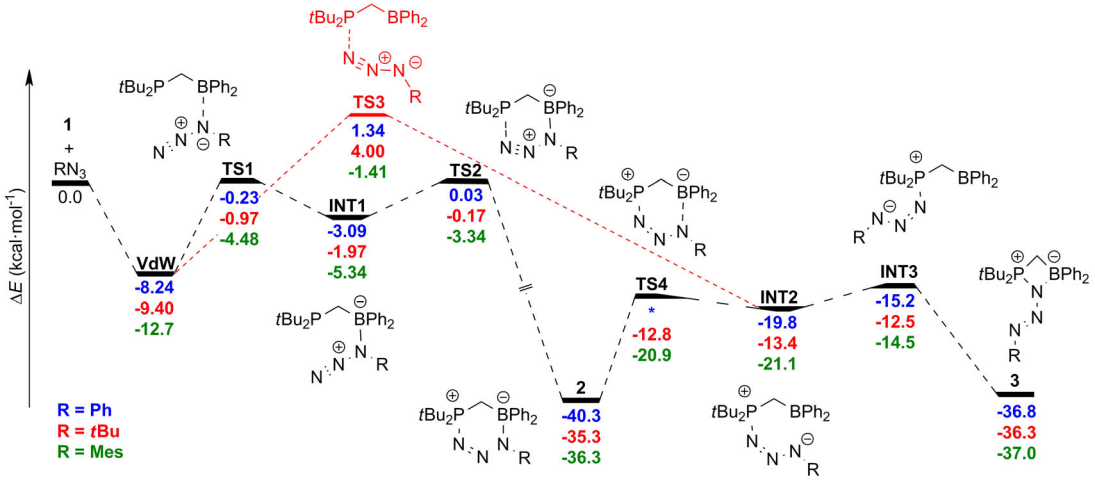

Scheme 2. Complete energy profile (ΔE) in kcal mol^{-1} for the formation of $\mathbf{2}_{Ph}$ (blue), $\mathbf{2}_{tBu}$ (red) and $\mathbf{2}_{Mes}$ (green) through initial P–N bond formation (interrupted Staudinger reaction, shown in red) versus initial B–N bond formation and rearrangement to heterocycle **3**. *$\mathbf{TS4}_{Ph}$ could not be located.

responding azide. The azide fragment in $\mathbf{3}_{t\mathrm{Bu}}$ and $\mathbf{3}_{\mathrm{Mes}}$ is attached to **1** with a *s-Z* conformation of the P1 and N3 moieties ($\mathbf{3}_{t\mathrm{Bu}}$: P1-N1-N2-N3 −1.66(19)°, $\mathbf{3}_{\mathrm{Mes}}$: P1-N1-N2-N3 0.000(1)°; Figure 2). The N1–N2 bond lengths ($\mathbf{3}_{t\mathrm{Bu}}$: 1.3573(16), $\mathbf{3}_{\mathrm{Mes}}$: 1.342(3) Å) are typical for a N–N single bond and the shorter N2–N3 distance ($\mathbf{3}_{t\mathrm{Bu}}$: 1.2502(17), $\mathbf{3}_{\mathrm{Mes}}$: 1.259(3) Å) resembles a N=N double bond, which matches well with the related adducts **D**.[14a–c] Monitoring of the reaction of **1** with *t*Bu–N_3 and Mes–N_3 by variable-temperature NMR spectroscopy revealed the presence of an intermediate during the reaction with comparable $^{31}P\{^1H\}$ and $^{11}B\{^1H\}$ NMR signals as observed for $\mathbf{2}_{\mathrm{Ph}}$ ($\mathbf{2}_{t\mathrm{Bu}}$: $\delta(^{31}P\{^1H\})=27.0$; $\delta(^{11}B\{^1H\})=-7.0$, $\mathbf{2}_{\mathrm{Mes}}$: $\delta(^{31}P\{^1H\})=40.5$; $\delta(^{11}B\{^1H\})=-6.7$ ppm), suggesting that the six-membered heterocycle is an intermediate in the formation of $\mathbf{3}_{t\mathrm{Bu}}$ and $\mathbf{3}_{\mathrm{Mes}}$.

DFT calculations indeed supported this hypothesis and we found that upon reacting **1** with *t*Bu–N_3 and Mes–N_3 the six-membered intermediates $\mathbf{2}_{t\mathrm{Bu}}$ and $\mathbf{2}_{\mathrm{Mes}}$ are easily accessible by B–N Lewis adduct formation and subsequent ring closure with maximum barriers of 9.2 and 9.4 kcal mol^{-1} (ΔE), respectively. All of the systems show a preference for initial B–N interaction over the Staudinger pathway that is a 1.9–4.2 kcal mol^{-1} higher energy process (*t*Bu–N_3 $\Delta E^{\ddagger}=13.4$, Mes–N_3 $\Delta E^{\ddagger}=11.3$ kcal mol^{-1}), but due to the small energetic differences it is possible that the initial P–N formation is also a minor competing process. In the case of phenyl azide, the six-membered heterocycle $\mathbf{2}_{\mathrm{Ph}}$ is the kinetic and thermodynamic product ($\Delta G_{6\text{-ring}}=-21.6$ vs. $\Delta G_{4\text{-ring}}=-19.7$ kcal mol^{-1}; see Figure 3 and Table 1), whereas with *tert*-butyl and mesityl substituents this heterocycle is only the kinetic product that can rearrange to the four-membered heterocycles $\mathbf{3}_{t\mathrm{Bu}}$ and $\mathbf{3}_{\mathrm{Mes}}$. When the steric bulk on the azide was reduced in silico (R = H, Table 1), more insight in the preference in ring formation was obtained: the formation of a 6-membered ring is most favored ($\Delta G_{6\text{-ring}}=-23.7$ kcal mol^{-1}), and the smaller the ring becomes, the less favored the formation is ($\Delta G_{5\text{-ring}}=-18.2$ (see below) vs. $\Delta G_{4\text{-ring}}=-15.8$ kcal mol^{-1}).

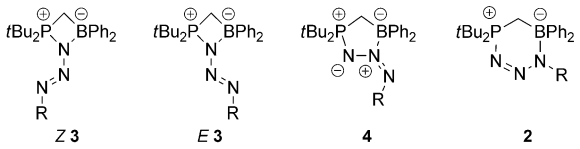

Figure 3. Four different isomers of FLP–azide adducts (R = H, Ph, *t*Bu, Mes, and TMS, see Table 1).

Table 1. The Gibbs free energy of formation of the three different adducts in kcal mol^{-1}; the lowest energy isomer in each case is highlighted.[a]

	6-ring (**2**)	4-ring *s-Z* (**3**)	5-ring (**4**)
1+HN_3	**−23.7**	−15.8	−18.2
1+PhN_3	**−21.6**	−19.7	−18.8
1+*t*BuN_3	−15.0	**−19.7**	−17.8
1+MesN_3	−15.1	−20.5	**−22.0**
1+TMSN_3	**−13.2**	−7.08	−11.4

[a] Calculated at the ωB97X-D/6-31G* level of theory.

For the follow up reaction, DFT calculations (ωB97X-D/6-31G*) showed that indeed the six-membered intermediate $\mathbf{2}_{t\mathrm{Bu}}$ (Scheme 2) can ring open by breaking the B–γ-N bond to form a phosphazide, $\mathbf{INT2}_{t\mathrm{Bu}}$,[26] which is the first intermediate of a Staudinger reaction. Subsequent rotation around the P–N σ-bond perfectly aligns the α-nitrogen of $\mathbf{INT3}_{t\mathrm{Bu}}$ for a barrierless ring closing to the α,α-nitrogen-coordinated four-membered heterocycle $\mathbf{3}_{t\mathrm{Bu}}$ (Scheme 2), which is the thermodynamic product. It should be noted that $\mathbf{INT2}_{t\mathrm{Bu}}$ can be formed directly from **1** and *t*Bu–N_3 through the Staudinger reaction, but the barrier for this process ($\Delta E^{\ddagger}=13.4$ kcal mol^{-1}) is higher than the barrier for the initial formation of $\mathbf{2}_{t\mathrm{Bu}}$ ($\Delta E^{\ddagger}=9.2$ kcal mol^{-1}), and thus the six-membered heterocycle is computed to be a likely intermediate in this transformation, consistent with the aforementioned NMR spectroscopic data. This process is also the preferred path for the rearrangement of $\mathbf{2}_{\mathrm{Mes}}$ into $\mathbf{3}_{\mathrm{Mes}}$.[27]

Interestingly, our computational analysis[28] revealed that for the reaction with mesityl azide the four-membered heterocycle $\mathbf{3}_{\mathrm{Mes}}$ is not the most stable isomer (Table 1). Indeed, heating a solution of $\mathbf{3}_{\mathrm{Mes}}$ in toluene at 75 °C for 3 days resulted in the formation of the thermodynamic product $\mathbf{4}_{\mathrm{Mes}}$ ($\delta(^{31}P\{^1H\})=91.6$; $\delta(^{11}B\{^1H\})=5.9$ ppm; Scheme 1), which is favored over $\mathbf{3}_{\mathrm{Mes}}$ by $\Delta G=-1.5$ kcal mol^{-1} (Figure 3) and most likely proceeds through the endothermic ring opening of $\mathbf{3}_{\mathrm{Mes}}$ to $\mathbf{INT3}_{\mathrm{Mes}}$ ($\Delta E=22.5$ kcal mol^{-1}). Single-crystal X-ray structure determination provided the molecular structure of $\mathbf{4}_{\mathrm{Mes}}$ (Figure 2, bottom right) which shows a five-membered heterocycle in which the FLP is attached to the α- and β-nitrogen of the azide, which is only the second example of such coordination mode for the reaction of an intramolecular frustrated Lewis pair with an organic azide[15] and highlights that for mesityl azide all three possible coordination modes are synthetically accessible. The P1–N1 and B1–N2 bond lengths (1.6592(13) [1.6557(13)], 1.668(2) [1.655(2)] Å, respectively) represent typical single bonds, and, similar to $\mathbf{3}_{t\mathrm{Bu}}$ and $\mathbf{3}_{\mathrm{Mes}}$, the N1–N2 bond is elongated (1.3364(17) [1.3397(17)] Å) compared with $\mathbf{2}_{\mathrm{Ph}}$, and the N2–N3 bond is shortened (1.2733(17) [1.2695)] Å), suggesting that resonance structure **3** (Figure 3) has a major contribution in this structure.

Next, we investigated the reactivity of *t*$Bu_2PCH_2BPh_2$ (**1**) with trimethylsilyl azide. Treatment of **1** with 1.1 equiv of TMS–N_3 at room temperature afforded complete conversion after six days to product **5**, which was isolated as a colorless solid in 89% yield ($\delta(^{31}P\{^1H\})=84.3$; $\delta(^{11}B\{^1H\})=3.2$ ppm; Scheme 3). The molecular structure of **5** revealed the formation of a four-membered heterocycle akin to **G** with only one azide N atom present; note that **5** can be regarded as a non-fluorinated analogue of the PCBN heterocycle reported by Stephan and coworkers, which is obtained from the reaction between a lithiated iminophosphorane and a chloroborane.[29] In **5**, the B1–N1 distance of 1.6802(18) Å is notably longer compared to the four-membered heterocycles $\mathbf{3}_{t\mathrm{Bu}}$ and $\mathbf{3}_{\mathrm{Mes}}$, indicating a weaker B1–N1 bond, likely due to steric hindrance. The P1–N1 distance is slightly shorter (1.6366(11) Å) and the nitrogen has a planar environment ($\Sigma=359°$), which suggest a pronounced phosphazene character of the P1–N1 bond. As **5** is obtained after elimination of dinitrogen, we were interested to find out

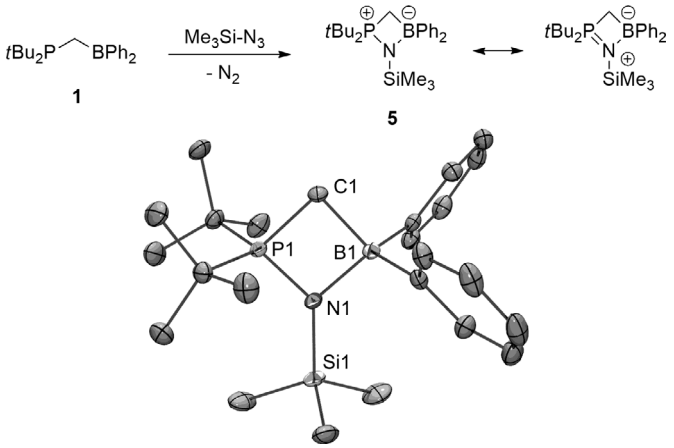

Scheme 3. The reaction of **1** with TMS–N_3 (top) and the molecular structure of **5** (bottom; ellipsoids at 50% probability, hydrogens are omitted for clarity). Selected bond lengths [Å] and angles [°] for **5**: P1–N1 1.6366(11), B1–N1 1.6802(18), N1–Si1 1.7348(12); P1-N1-B1 90.96(7), B1-N1-Si1 132.33(8), Si1-N1-P1 135.66(7).

how it is formed. During the reaction, one intermediate was observed by ^{31}P and ^{11}B NMR spectroscopy with similar chemical shifts as observed for **2** (R = Ph, *t*Bu, Mes) ($\delta(^{31}P\{^1H\}) = 26.7$; $\delta(^{11}B\{^1H\}) = -9.9$ ppm), therefore we postulate that the six-membered heterocycle $\mathbf{2_{TMS}}$ is an intermediate in the formation of **5**. DFT calculations support this notion and revealed that the formation of $\mathbf{2_{TMS}}$ via $\mathbf{INT1_{TMS}}$ is a low-energy process ($\Delta E^{\ddagger} = 9.8$, $\Delta E = -24.2$ kcal mol^{-1}), which is in good agreement with our spectroscopic findings.[26] We were able to locate a transition state for direct N_2 elimination from $\mathbf{INT1_{TMS}}$, which is comparable to the thermal elimination of N_2 from diarylazidoboranes (see page S72, Supporting Information).[30] However, this process is too high in energy ($\Delta E^{\ddagger} = 37.3$, $\Delta G^{\ddagger} = 44.2$ kcal mol^{-1}) to proceed at room temperature and was therefore regarded as unfeasible. We postulate that the elimination of N_2 proceeds through ring opening of $\mathbf{2_{TMS}}$ by breaking the B–N bond that affords intermediate $\mathbf{INT2_{TMS}}$, which eliminates dinitrogen through a classical Staudinger mechanism to form the corresponding iminophosphorane followed by ring closure to form **5** (Scheme 3), yet the transition states for this process could not be located on the potential-energy surface. Alternatively, Schulz and co-workers found that elimination of N_2 could proceed via a structure comparable to **INT1**.[24c] However, such mechanism would presumably lead to a different product than **5**.[31] Related compounds have been referred to as formal FLP adducts of nitrenes.[18] Based on this finding of N_2 loss in the TMS–N_3 reactions, we explored the possibility of similar N_2 extrusion for the Ph-, *t*Bu- and Mes-substituted azide products; according to DFT calculations, N_2 loss is thermodynamically favorable in all cases (see Table S1 in the Supporting Information). However, $\mathbf{3_{tBu}}$ and $\mathbf{4_{Mes}}$ are both thermally stable up to 100 °C when dissolved in toluene, whereas $\mathbf{2_{Ph}}$ decomposes unselectively to a range of products.

To investigate the follow-up chemistry of **5**, we first targeted removal of the TMS group, in analogy to the related carbene–nitrene adducts **C** (Figure 1).[12] Unfortunately, treatment of **5** with 1 equiv of ethanol resulted in the formation of multiple unidentifiable products. More successful was the reaction of **5** with 1 equiv of HCl (2 M in Et_2O) at −78 °C, which led to the selective formation of a new product **6**, which shows only marginally different signals in the $^{31}P\{^1H\}$ and $^{11}B\{^1H\}$ NMR spectrum ($\delta(^{31}P\{^1H\}) = 78.1$; $\delta(^{11}B\{^1H\}) = 2.4$ ppm) compared to **5**, and an additional doublet for a N–H proton in the ^{1}H NMR spectrum ($\delta(^1H) = 4.68$ ppm, $^2J_{H,P} = 12.6$ Hz). We postulate **5** to behave as a "masked FLP" capturing HCl by ring opening, comparable to the P/Al and P/B FLPs reported by Uhl and Erker,[32,33] which leads to protonation of the phosphazene moiety and chloride addition to the borane giving compound **6** (Scheme 4). The formation of **6** is further supported by the detection of the $[\mathbf{6}-Cl]^+$ cation by high-resolution mass spectrometry.

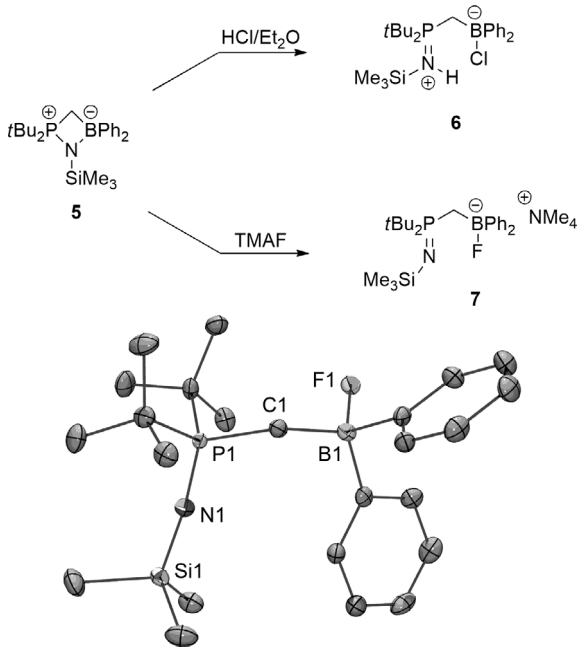

Scheme 4. The reaction of **5** with HCl and TMAF (top) and the molecular structure of **7** (bottom; ellipsoids at 50% probability, hydrogens Me_4N cation and a second ion pair of **7** are omitted for clarity). Selected bond lengths [Å] and angles [°] for **7** (structural parameter for the second crystallographic independent molecule in brackets): P1–N1 (1.543(3) [1.545(3)], B1–F1 1.470(4) [1.473(4)], N1–Si1 1.653(3) [1.648(3)]; P1-C1-B1 131.9(2) [130.9(2)], P1-N1-Si1 171.5(2) [174.6(2)], Σ(C-B1-C) 331 [332]).

To investigate the ring-opening behavior of **5** in more detail, we reacted **5** with an equimolar amount of anhydrous tetramethylammonium fluoride (TMAF) in MeCN/THF at 0 °C, which afforded the ring-opened product **7**. The $^{31}P\{^1H\}$ NMR spectrum displayed a singlet at 38.2 ppm, and the $^{11}B\{^1H\}$ NMR spectrum showed a characteristic doublet due to a $^1J_{B,F}$ coupling at $\delta(^{11}B\{^1H\}) = 2.35$ ppm with $^1J_{B,F} = 48.6$ Hz indicating that the fluoride is directly attached to the borane moiety. As final proof, a single-crystal X-ray structure determination confirmed the molecular structure of **7**, which displays a slightly shortened P1–N1 bond (1.543(3) [1.545(3)] Å) compared with **5** and an almost linear orientation of the P1-N1-Si1 bond angle (171.5(2)° [174.6(2)°]; Scheme 4), which is relatively large for such P=N–Si motif, but observed previously for electron rich phosphines.[34]

To further probe the reactivity of **5** as a "masked" frustrated Lewis pair, ωB97X-D/6-31G* calculations revealed that the splitting of the boron–nitrogen bond creating iminophosphorane/borane based FLP **5′** is only slightly uphill ($\Delta G = 5.53$, $\Delta E = 9.48$ kcal mol^{-1}; Scheme 5) and is comparable to the energy required for ring opening of the four-membered heterocyclic P/B FLP reported by Erker and co-workers ($\Delta E \approx 7$ kcal mol^{-1}).[33] We found that **5** is indeed susceptible to undergo reactions with typical FLP substrates, such as isocyanates.

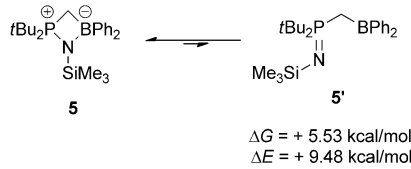

Scheme 5. The equilibrium between the open (**5′**) and closed form of **5** and the corresponding energies.

Specifically, treatment of **6** with an excess (14.4 equiv) of phenylisocyanate in THF at 60 °C for three days resulted in the formation of insertion product **8** ($\delta(^{31}P\{^1H\}) = 57.1$; $\delta(^{11}B\{^1H\}) = -3.1$ ppm; Scheme 6),[14a,e,16,19a,32b,35] which represents a rare

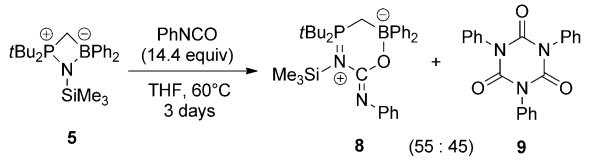

Scheme 6. The reaction of **5** with phenylisocyanate.

case of an FLP using a iminophosphorane as Lewis base.[36] Next to the formation of **8**, full NMR analysis of the product revealed the formation of a second product in a 55:45 ratio (**8**:**9**), which was characterized as the cyclo-trimerization product **9**. Although the cyclo-oligomerization of isocyanates is known to be catalyzed by Lewis bases, such as NHCs,[37] amines,[38] Verkade's bases[39] and phosphines,[40] or phosphides,[41] this represents to our knowledge the first example of cyclo-oligomerization of phenylisocyanate in which a (masked) frustrated Lewis pair is involved.

Conclusions

We have shown that the phosphorus/boron-based FLP tBu$_2$PCH$_2$BPh$_2$ (**1**) reacts with tBu–N$_3$, Mes–N$_3$ and Ph–N$_3$ giving four-, five-, and six-membered heterocycles, respectively. The mechanism was studied by DFT calculations, which revealed that instead of a Staudinger reaction, the reaction starts with formation of a B–N Lewis adduct (**INT1**), which ring closes to form the six-membered heterocycle **2**. In case of the bulkier tBu–N$_3$ and Mes–N$_3$, **2** is the kinetic product that can subsequently rearrange to the thermodynamically most stable isomer. DFT calculations and NMR spectroscopy suggest that reaction of **1** with TMS–N$_3$ follows the same mechanism, however the six-membered intermediate is unstable and rapid extrusion of dinitrogen results in full conversion towards the four-membered heterocycle **5**. Compound **5** is reactive, and was found to ring open upon treatment with hydrochloric acid or tetramethylammonium fluoride. Additionally, **5** also retained FLP reactivity when reacted with phenylisocyanate, resulting in PhNCO addition creating a new six-membered heterocycle. At the same time, **5** can promote the cyclo-trimerization of phenylisocyanate to the corresponding isocyanurate.

Experimental Section

General methods and materials

All manipulations were carried out under an atmosphere of dry nitrogen, using standard Schlenk and drybox techniques, and were performed in the dark as a precaution to prevent decomposition. Solvents were purified, dried, and degassed according to standard procedures. ^{1}H and $^{13}C\{^1H\}$ NMR spectra were recorded on a Bruker Avance 400 spectrometer and internally referenced to the residual solvent resonances ([D$_8$]THF: ^{1}H: $\delta = 3.58$, 1.72, $^{13}C\{^1H\}$: $\delta = 67.2$, 25.3; CD$_2$Cl$_2$: ^{1}H: $\delta = 5.32$, $^{13}C\{^1H\}$: $\delta = 53.8$ ppm). $^{31}P\{^1H\}$ and $^{11}B\{^1H\}$ NMR spectra were recorded on a Bruker Avance 400 spectrometer and externally referenced (85% H_3PO_4, $BF_3{\cdot}OEt_2$, respectively). ^{19}F NMR spectra were recorded on a Bruker AV300-II and externally referenced ($CFCl_3$). Chemical shifts are reported in ppm. Melting points were measured on a Büchi M-565 melting point apparatus in sealed capillaries and are uncorrected. High-resolution mass spectra were recorded on a Bruker MicroTOF with ESI nebulizer (ESI), or on an AccuTOF GC v 4 g, JMS-T100GCV, Mass spectrometer (JEOL, Japan) with a LiFDi probe (FD/FI) equipped with a FD Emitter, Linden CMS GmbH (Germany), FD 13 μm. Current rate 51.2 mA min^{-1} over 1.2 min and typical measurement conditions are: counter electrode −10 kV, ion source 37 V. Trimethylsilyl azide (TMS–N$_3$), hydrochloric acid 2 M in diethyl ether (HCl/Et$_2$O) and phenyl isocyanate (PhNCO) were purchased from commercial resources. TMS–N$_3$ and PhNCO were stored over molecular sieves (4 Å), and HCl/Et$_2$O (2 M) was used as received. tBu–N$_3$,[42] Ph–N$_3$,[43] Mes–N$_3$,[44] anhydrous tetramethylammonium fluoride (TMAF)[45] and tBu$_2$PCH$_2$BPh$_2$[19a] were prepared following literature procedures.

Synthesis and characterization

Synthesis of 2$_{Ph}$: Phenyl azide (0.074 g, 0.617 mmol, 1.0 equiv) was added to a solution of tBu$_2$PCH$_2$BPh$_2$ (**1**; 0.200 g, 0.617 mmol, 1.0 equiv) in THF (10 mL) at −10 °C. After addition, the reaction mixture was stirred for 10 minutes at −10 °C, after which it was allowed to warm to room temperature and stirred for another 10 minutes. Removal of the solvent and subsequent washing with n-pentane (3×10 mL) gave **2$_{Ph}$** as a yellow solid (0.267 g, 98%). X-ray quality crystals were grown at room temperature from a THF/toluene solvent mixture layered with n-pentane. M.p. (nitrogen, sealed capillary): 121 °C (decomp); ^{1}H NMR (400.1 MHz, [D$_8$]THF, 293 K): $\delta = 7.26$ (d, $^3J_{H,H} = 6.9$ Hz, 4H; o-BC$_6H_5$), 7.09 (d, $^3J_{H,H} = 7.3$ Hz, 2H; o-NC$_6H_5$), 7.04 (t, $^3J_{H,H} = 7.4$ Hz, 4H; m-BC$_6H_5$), 6.95–6.84 (m, 5H; m-NC$_6H_5$, p-BC$_6H_5$, and p-NC$_6H_5$), 1.81 (d, $^2J_{H,P} = 12.0$ Hz, 2H; PCH_2B), 1.22 ppm (d, $^3J_{H,P} = 14.3$ Hz, 18H; PC(CH_3)$_3$); $^{13}C\{^1H\}$ NMR (100.6 MHz, [D$_8$]THF, 293 K): $\delta = 153.2$ (only observed in the HMBC spectrum, $^2J_{C,H}$ coupling with o-BC$_6H_5$, $^3J_{C,H}$ coupling with m-BC$_6H_5$ and PCH_2B; $ipso$-BC$_6$H$_5$), 150.0 (s; $ipso$-NC$_6$H$_5$), 134.8, (s; o-BC$_6$H$_5$),

127.5 (s; *m*-BC_6H_5), 127.4 (s; *m*-NC_6H_5), 125.3 (s; *p*-NC_6H_5), 125.2 and 125.1 (2x s; *p*-BC_6H_5 and *o*-NC_6H_5), 36.0 (d, $^1J_{C,P}=50.5$ Hz; P*C*(CH_3)$_3$), 26.6 (s; PC(CH_3)$_3$), 12.7 ppm (only observed in the HSQC spectrum, $^1J_{C,H}$ coupling with PCH_2B; PCH_2B); $^{31}P\{^1H\}$ NMR (162.0 MHz, [D_8]THF, 294 K): $\delta=31.8$ ppm (s). $^{11}B\{^1H\}$ NMR (128.4 MHz, [D_8]THF, 294 K): $\delta=-6.8$ ppm (s); HR ESI-MS: calcd for $C_{27}H_{35}BN_3PK$ (M+K) 482.2293, found 482.2309.

Synthesis of $\mathbf{3}_{tBu}$: *tert*-Butyl azide (0.081 g, 0.817 mmol, 1.1 equiv) was added to a solution of *t*$Bu_2PCH_2BPh_2$ (**1**; 0.241 g, 0.743 mmol, 1.0 equiv) in THF (10 mL) at 0 °C. After addition, the reaction mixture was allowed to warm to room temperature after which it was stirred overnight. Removal of the solvent and subsequent washing with *n*-pentane (3×8 mL) gave $\mathbf{3}_{tBu}$ as a colorless solid (0.221 g, 70%). X-ray quality crystals were grown at room temperature by vapor diffusion of *n*-pentane into a solution of $\mathbf{3}_{tBu}$ in THF. M.p. (nitrogen, sealed capillary): 126 °C (decomp); ^1H NMR (400.1 MHz, [D_8]THF, 297 K): $\delta=7.49$ (d, $^3J_{H,H}=7.3$ Hz, 4H; *o*-C_6H_5), 7.00 (t, $^3J_{H,H}=7.4$ Hz, 4H; *m*-C_6H_5), 6.84 (t, $^3J_{H,H}=7.3$ Hz, 2H; *p*-C_6H_5), 1.44 (d, $^2J_{H,P}=11.0$ Hz, 2H; PCH_2B), 1.34 (s, 9H; NC(CH_3)$_3$), 1.24 ppm (d, $^3J_{H,P}=15.3$ Hz, 18H; PC(CH_3)$_3$); $^{13}C\{^1H\}$ NMR (100.6 MHz, [D_8]THF, 297 K): $\delta=156.5$ (only observed in the HMBC spectrum, $^2J_{C,H}$ coupling with *o*-C_6H_5, $^3J_{C,H}$ coupling with *m*-C_6H_5 and PCH_2B; *ipso*-C_6H_5), 131.5 (s; *o*-C_6H_5), 127.0 (s; *m*-C_6H_5), 124.1 (s; *p*-C_6H_5), 61.7 (s; N*C*(CH_3)$_3$), 37.6 (d, $^1J_{C,P}=25.6$ Hz; P*C*(CH_3)$_3$), 28.7 (s; NC(*C*H_3)$_3$), 28.1 (d, $^3J_{H,P}=2.7$ Hz, 18H; PC(*C*H_3)$_3$), 6.7 ppm (only observed in the HSQC spectrum, $^1J_{C,H}$ coupling with PCH_2B; PCH_2B); $^{31}P\{^1H\}$ NMR (162.0 MHz, [D_8]THF, 293 K): $\delta=95.5$ ppm (s); $^{11}B\{^1H\}$ NMR (128.4 MHz, [D_8]THF, 294 K): $\delta=2.9$ ppm (s); HR ESI-MS: calcd for $C_{25}H_{40}BN_3P$ (M+H) 424.3047, found 424.3044; calcd for $C_{25}H_{39}BN_3PK$ (M+K) 462.2606, found 462.2611.

Synthesis of $\mathbf{3}_{Mes}$: Mesitylazide (0.133 g, 0.823 mmol, 1.0 equiv) was added to a solution of *t*$Bu_2PCH_2BPh_2$ (**1**; 0.267 g, 0.823 mmol, 1.0 equiv) in THF (12 mL) at 0 °C. After addition, the reaction mixture was allowed to warm to room temperature after which it was stirred for 1 hour. Removal of the solvent and subsequent washing with *n*-pentane (3×3 mL) gave $\mathbf{3}_{Mes}$ as a pale white solid in 80% yield (0.320 g, 0.659 mmol). X-ray quality crystals were grown at room temperature from a solution of $\mathbf{3}_{Mes}$ in THF layered with *n*-pentane. M.p. (nitrogen, sealed capillary): 175 °C (decomp); ^1H NMR (400.1 MHz, [D_8]THF, 297 K): $\delta=7.53$ (d, $^3J_{H,H}=7.3$ Hz, 4H; *o*-C_6H_5), 7.01 (t, $^3J_{H,H}=7.4$ Hz, 4H; *m*-C_6H_5), 6.88 (s, 2H; *m*-Mes*H*), 6.86 (t, $^3J_{H,H}=7.3$ Hz, 2H; *p*-C_6H_5), 2.27 (s, 3H; *p*-MesCH_3), 2.25 (s, 6H; *o*-MesCH_3), 1.62 (d, $^2J_{H,P}=11.0$ Hz, 2H; PCH_2B), 1.35 ppm (d, $^3J_{H,P}=15.4$ Hz, 18H, PC(CH_3)$_3$); $^{13}C\{^1H\}$ NMR (100.6 MHz, [D_8]THF, 297 K): $\delta=156.0$ (only observed in the HMBC spectrum, $^2J_{C,H}$ coupling with *o*-C_6H_5, $^3J_{C,H}$ coupling with *m*-C_6H_5 and PCH_2B; *ipso*-C_6H_5), 147.5 (s; *ipso*-Mes*C*), 135.4 (s; *p*-Mes*C*), 131.7 (s; *o*-C_6H_5), 130.3 (s; *o*-Mes*C*), 129.9 (s; *m*-Mes*C*), 127.1 (s; *m*-C_6H_5), 124.2 (s; *p*-C_6H_5), 37.9 (d, $^1J_{C,P}=24.9$ Hz; P*C*(CH_3)$_3$), 28.0 (d, $^2J_{C,P}=1.8$ Hz; PC(CH_3)$_3$), 20.7 (s; *p*-MesCH_3), 19.8 (s; *o*-MesCH_3), 6.50 ppm (only observed in the HSQC spectrum, $^1J_{C,H}$ coupling with PCH_2B; PCH_2B); $^{31}P\{^1H\}$ NMR (162.0 MHz, [D_8]THF, 297 K): $\delta=98.3$ ppm (s); $^{11}B\{^1H\}$ NMR (128.4 MHz, [D_8]THF, 297 K): $\delta=3.8$ ppm (s); HR ESI-MS: calcd for $C_{30}H_{42}BN_3P$ (M+H) 486.3204, found 486.3215; calcd for $C_{30}H_{41}BN_3PK$ (M+K) 524.2763, found 524.2757.

Rearrangement of $\mathbf{3}_{Mes}$ to $\mathbf{4}_{Mes}$: Mesitylazide-FLP adduct $\mathbf{3}_{Mes}$ (0.043 g, 0.089 mmol) was dissolved in toluene (10 mL), heated to 75 °C and stirred for 66 hours at this reaction temperature. Subsequently, the solvent was removed in vacuo and the product was dissolved a mixture of *n*-pentane (8 mL) and THF (1 mL). The solution was filtered and stored at −20 °C for 4 days and then 1 day at −80 °C, after which crystals had formed. The mother liquor was filtered off and after removal of the solvent $\mathbf{4}_{Mes}$ was obtained as a colorless solid (0.031 g, 73%). X-ray quality crystals were grown by cooling a saturated solution of $\mathbf{4}_{Mes}$ in a THF/*n*-pentane mixture to −20 °C. M.p. (nitrogen, sealed capillary): 203 °C (decomp); ^1H NMR (400.1 MHz, [D_8]THF, 297 K): $\delta=7.66$ (d, $^3J_{H,H}=7.4$ Hz, 4H; *o*-C_6H_5), 7.07 (t, $^3J_{H,H}=7.4$ Hz, 4H; *m*-C_6H_5), 6.96 (t, $^3J_{H,H}=7.2$ Hz, 2H; *p*-C_6H_5), 6.74 (s, 2H; *m*-Mes*H*), 2.21 (s, 3H; *p*-MesCH_3), 2.00 (d, $^2J_{H,P}=11.9$ Hz, 2H; PCH_2B), 1.90 (s, 6H; *o*-MesCH_3), 1.20 ppm (d, $^3J_{H,P}=14.4$ Hz, 18H, PC(CH_3)$_3$); $^{13}C\{^1H\}$ NMR (100.6 MHz, [D_8]THF, 297 K): $\delta=152.5$ (only observed in the HMBC spectrum, $^2J_{C,H}$ coupling with *o*-C_6H_5, $^3J_{C,H}$ coupling with *m*-C_6H_5 and PCH_2B; *ipso*-C_6H_5), 147.5 (s; *ipso*-Mes*C*), 134.1 (s; *p*-Mes*C*), 133.0 (s; *o*-C_6H_5), 128.8 (s; *m*-Mes*C*), 128.6 (s; *o*-Mes*C*), 126.9 (s; *m*-C_6H_5), 125.3 (s; *p*-C_6H_5), 35.5 (d, $^1J_{C,P}=49.0$ Hz; P*C*(CH_3)$_3$), 26.9 (s; PC(*C*H_3)$_3$), 20.8 (s; *p*-MesCH_3), 18.7 (s; *o*-MesCH_3), 7.70 ppm (only observed in the HSQC spectrum, $^1J_{C,H}$ coupling with PCH_2B; PCH_2B); $^{31}P\{^1H\}$ NMR (162.0 MHz, [D_8]THF, 297 K): $\delta=91.6$ ppm (s); $^{11}B\{^1H\}$ NMR (128.4 MHz, [D_8]THF, 297 K): $\delta=6.1$ ppm (s).

Synthesis of 5: Trimethylsilyl azide (0.088 g, 0.101 mL, 0.763 mmol, 1.1 equiv) was added to a solution of *t*$Bu_2PCH_2BPh_2$ (**1**; 0.225 g, 0.694 mmol, 1.0 equiv) in THF (12 mL) at 0 °C. After addition, the reaction mixture allowed to warm to room temperature after which it was stirred for 6 days. Removal of the solvent in vacuo gave **5** as a colorless solid (0.271 g, 89%). If necessary, the product was washed with cold *n*-pentane (0 °C) to remove impurities. X-ray quality crystals were grown by cooling a saturated solution of **5** in *n*-pentane to −20 °C. M.p. (nitrogen, sealed capillary): 94 °C (decomp); ^1H NMR (400.1 MHz, [D_8]THF, 293 K): $\delta=7.36$ (d, $^3J_{H,H}=7.3$ Hz, 4H; *o*-C_6H_5), 7.02 (t, $^3J_{H,H}=7.4$ Hz, 4H; *m*-C_6H_5), 6.91 (t, $^3J_{H,H}=7.2$ Hz, 2H; *p*-C_6H_5), 1.52 (d, $^2J_{H,P}=11.7$ Hz, 2H; PCH_2B), 1.33 ppm (d, $^3J_{H,P}=14.3$ Hz, 18H; PC(CH_3)$_3$), 0.23 (s, 9H; Si(CH_3)$_3$); $^{13}C\{^1H\}$ NMR (100.6 MHz, [D_8]THF, 293 K): $\delta=156.1$ (only observed in the HMBC spectrum, $^2J_{C,H}$ coupling with *o*-C_6H_5, $^3J_{C,H}$ coupling with *m*-C_6H_5 and PCH_2B; *ipso*-C_6H_5), 133.9 (s; *o*-C_6H_5), 126.5 (s; *m*-C_6H_5), 124.5 (s; *p*-C_6H_5), 38.0 (d, $^1J_{C,P}=33.1$ Hz; P*C*(CH_3)$_3$), 28.2 (d, $^2J_{C,P}=2.7$ Hz; PC(CH_3)$_3$), 10.3 (only observed in the HSQC spectrum, $^1J_{C,H}$ coupling with PCH_2B; PCH_2B), 5.1 ppm (s; Si(CH_3)$_3$); $^{31}P\{^1H\}$ NMR (162.0 MHz, [D_8]THF, 293 K): $\delta=84.3$ (s); $^{11}B\{^1H\}$ NMR (128.4 MHz, [D_8]THF, 294 K): $\delta=3.2$ ppm (s); HR ESI-MS**:** calcd for $C_{24}H_{40}BNPSi$ (M+H) 412.2755, found 412.2786.

Synthesis of 6: A solution of HCl (2 M in Et_2O, 0.26 mL, 0.52 mmol, 1.0 equiv) was added dropwise to a solution of **5** in THF (8 mL) at −78 °C. After addition, the mixture was stirred for 5 minutes at −78 °C and was subsequently warmed to room temperature. The solvent was removed in vacuo to afford a colorless solid that was washed with *n*-pentane (3×4 mL) and subsequently dried in vacuo to yield **6** as a colorless solid (0.189 g, 81%). M.p. (nitrogen, sealed capillary): 93 °C (decomp); ^1H NMR (400.1 MHz, CD_2Cl_2, 298 K): $\delta=7.46$ (d, $^3J_{H,H}=7.5$ Hz, 4H; *o*-C_6H_5), 7.16 (t, $^3J_{H,H}=7.4$ Hz, 4H; *m*-C_6H_5), 7.05 (t, $^3J_{H,H}=7.2$ Hz, 2H; *p*-C_6H_5), 4.68 (d, $^2J_{H,P}=12.7$ Hz, 1H; N*H*), 1.86 (d, $^2J_{H,P}=11.1$ Hz, 2H; PCH_2B), 1.23 (d, $^3J_{H,P}=14.7$ Hz, 18H; PC(CH_3)$_3$), 0.28 ppm (s, 9H; Si(CH_3)$_3$); ^{13}C $\{^1H\}$ NMR (100.6 MHz, CD_2Cl_2, 300 K): δ 133.2 (s; *o*-C_6H_5), 127.1 (s; *m*-C_6H_5), 125.1 (s; *p*-C_6H_5), 36.5 (d, $^1J_{C,P}=49.0$ Hz; P*C*(CH_3)$_3$), 27.6 (s; PC(*C*H_3)$_3$), 14.8 (only observed in the HSQC spectrum, $^1J_{C,H}$ coupling with PCH_2B; PCH_2B), 2.27 ppm (d, $^3J_{C,P}=1.4$ Hz; Si(CH_3)$_3$), the signal for *ipso*-C_6H_5 is unresolved; $^{31}P\{^1H\}$ NMR (162.0 MHz, CD_2Cl_2, 298 K): $\delta=78.1$ ppm (s); $^{11}B\{^1H\}$ NMR (128.4 MHz, CD_2Cl_2, 299 K): $\delta=2.4$ ppm (s); HR LiFDI-MS**:** calcd for $C_{24}H_{40}BNPSi$ (M−Cl) 412.2755, found 412.2750.

Synthesis of 7: A solution of anhydrous tetramethylammonium fluoride (0.0454 g, 0.487 mmol, 1.0 equiv) in MeCN (10 mL) was added to a solution of **5** (0.200 g, 0.486 mmol, 1.0 equiv) in THF (15 mL) at 0 °C. After addition, the reaction mixture was warmed to room temperature and stirred for 1 hour. Removal of the solvent

and subsequent washing with *n*-pentane (3×8 mL) gave **7** as a white solid, which was subsequently washed with benzene (3× 8 mL) to afford **7** as a pure, colorless solid (0.178 g, 73%). X-ray quality crystals were grown at room temperature from a solution of **7** in THF layered with *n*-pentane. M.p. (nitrogen, sealed capillary): 118 °C (decomp); ^{1}H NMR (400.1 MHz, CD_2Cl_2, 298 K): $\delta = 7.57$ (d, $^3J_{H,H} = 6.9$ Hz, 4H; *o*-C_6H_5), 7.08 (t, $^3J_{H,H} = 7.3$ Hz, 4H; *m*-C_6H_5), 6.90 (t, $^3J_{H,H} = 7.2$ Hz, 2H; *p*-C_6H_5), 1.31–1.19 (m, 2H; PCH_2B), 1.11 (d, $^3J_{H,P} = 12.6$ Hz, 18H; PC(CH_3)$_3$), −0.18 ppm (s, 9H; Si(CH_3)$_3$); ^{13}C{^{1}H} NMR (100.6 MHz, CD_2Cl_2, 300 K): $\delta = 132.2$ (d, $^3J_{C,F} = 6.7$ Hz; *o*-C_6H_5), 126.7 (s; *m*-C_6H_5), 123.2 (s; *p*-C_6H_5), 36.2 (d, $^1J_{C,P} = 60.3$ Hz; PC(CH$_3$)$_3$), 28.2 (m; PC(CH_3)$_3$), 22.9 (only observed in the HSQC spectrum, $^1J_{C,H}$ coupling with PCH_2B; PCH_2B), 4.9 ppm (s; Si(CH_3)$_3$), the signal for *ipso*-C_6H_5 is unresolved; ^{31}P{^{1}H} NMR (162.0 MHz, CD_2Cl_2, 298 K): $\delta = 38.2$ ppm (s); ^{11}B{^{1}H} NMR (128.4 MHz, CD_2Cl_2, 299 K): $\delta = 2.4$ ppm (d, $^1J_{B,F} = 48.6$ Hz); ^{19}F NMR (282.4 MHz, CD_2Cl_2, 299 K): $\delta = -191.7$ ppm (br. s); HR ESI-MS: calcd for $C_{24}H_{39}BFNPSi$ (M−Me$_4$N) 430.2672, found 430.2673.

Synthesis of 8 and 9: PhNCO (2.786 g, 2.54 mL, 23.39 mmol, 14.4 equiv) was added to a solution of **5** (0.673 g, 1.636 mmol, 1.0 equiv) in THF (45 mL) at room temperature. After addition, the reaction mixture was warmed to 60 °C and stirred for 3 days at this temperature. The solvent and excess PhNCO were removed in vacuo to afford a pale white solid, which was washed at 0 °C with *n*-pentane (3×8 mL). Subsequent drying in vacuo afforded a pale white solid that consists of a mixture of the product (**8**) and phenyl isocyanurate (**9**) in 55:45 ratio (0.967 g). Compound **8:** ^{1}H NMR (400.1 MHz, CD_2Cl_2, 299 K): $\delta = 7.33$ (d, $^3J_{H,H} = 7.1$ Hz, 4H; *o*-BC_6H_5), 7.06 (t, $^3J_{H,H} = 7.4$ Hz, 4H; *m*-BC_6H_5), 6.96, (t, $^3J_{H,H} = 7.2$ Hz, 2H; *p*-BC_6H_5), 6.88–6.08 (br. m, 4H; *o*,*m*-NC_6H_5), 6.77–6.71 (m, 1H; *p*-NC_6H_5), 1.61 (d, $^2J_{H,P} = 10.9$ Hz, 2H; PCH_2B), 1.16 (d, $^3J_{H,P} = 14.2$ Hz, 18H; PC(CH_3)$_3$, 0.26 ppm (s, 9H; Si(CH_3)$_3$); ^{13}C{^{1}H} NMR (100.6 MHz, CD_2Cl_2, 299 K): $\delta = 146.4$ (s; *ipso*-NC_6H_5), 134.4 (s; *o*-BC_6H_5), 128.0 and 127.0 (s; *o*-NC_6H_5 and *m*-NC_6H_5), 126.8 (s; *m*-BC_6H_5), 124.4 (s; *p*-BC_6H_5), 123.5 (s; *p*-NC_6H_5), 35.8 (d, $^1J_{C,P} = 57.3$ Hz; PC(CH$_3$)$_3$), 26.8 (s; PC(CH_3)$_3$), 14.6 (only observed in the HSQC spectrum, $^1J_{C,H}$ coupling with PCH_2B; PCH_2B), 0.71 ppm (s; Si(CH_3)$_3$), the signals for *ipso*-BC_6H_5 and NCO are unresolved; ^{31}P{^{1}H} NMR (162.0 MHz, CD_2Cl_2, 298 K): $\delta = 56.5$ ppm (s); ^{11}B{^{1}H} NMR (128.4 MHz, CD_2Cl_2, 298 K): $\delta = -3.4$ ppm (s); HR ESI-MS: calcd for $C_{31}H_{45}BN_2OPSi$ (M+H) 531.3126, found 531.3142. Compound **9:** ^{1}H NMR (400.1 MHz, CD_2Cl_2, 299 K): $\delta = 7.58$–7.47 (m, 9H; *m*,*p*-C_6H_5), 7.41 ppm (d, $^3J_{H,H} = 7.6$ Hz, 6H; *o*-C_6H_5); ^{13}C{^{1}H} NMR (100.6 MHz, CD_2Cl_2, 299 K): $\delta = 149.1$ (s; *ipso*-C_6H_5), 134.4 (*s*; *C*O), 129.84, (s; *m*-C_6H_5), 129.79 (s; *p*-C_6H_5), 128.9 ppm (s; *o*-C_6H_5).

X-ray crystal structure determinations

The single-crystal X-ray diffraction studies were carried out on a Bruker D8 Venture diffractometer with Photon100 detector at 123(2) K using Cu-Kα radiation ($\lambda = 1.54178$ Å) (**2$_{Ph}$**), or Bruker D8 Venture diffractometer with PhotonII CPAD detector at 123(2) K using Cu-Kα radiation ($\lambda = 1.54178$ Å) (**7**) or Bruker D8 Venture diffractometer with Photon100 detector at 123(2) K using Mo-Kα radiation ($\lambda = 0.71073$ Å) (**3$_{tBu}$**, **3$_{Mes}$**, **4$_{Mes}$**, **5**). Direct Methods (SHELXS-97)[46] (for **2$_{Ph}$**, **3$_{tBu}$**, **3$_{Mes}$**, **4$_{Mes}$**, **5**) and Dual Space methods (SHELXT)[47] (for **7**) were used for structure solution and refinement was carried out using SHELXT-2013/2014 (full-matrix least-squares on F^2).[48] Hydrogen atoms were localized by difference electron density determination and refined using a riding model. Semi-empirical absorption corrections were applied. **2$_{Ph}$** and **7** were refined as an inversion twin, for **3$_{Mes}$** the absolute structure was determined.[49] For **3**t_{Bu} and **4$_{Mes}$** an extinction correction was applied. In **7** one Me_4N^+ cation is disordered (see cif-file for details).[50]

2$_{Ph}$: colorless crystals, $C_{27}H_{35}BN_3P$, $M_r = 443.36$, crystal size 0.20×0.10×0.06 mm, orthorhombic, space group *Pca*2$_1$ (no.29), $a = 20.3505(5)$, $b = 18.8682(5)$, $c = 12.8093(3)$ Å, $V = 4918.5(2)$ Å^3, $Z = 8$, $\rho = 1.197$ Mg m^{-1-3}, μ(Cu-K$_\alpha$) = 1.12 mm^{-1}, $F(000) = 1904$, $2\theta_{max} = 144.0°$, 36741 reflections, of which 9434 were independent ($R_{int} = 0.039$), 578 parameters, 1 restraint, $R1 = 0.034$ (for 8901 $I > 2\sigma(I)$), $wR2 = 0.086$ (all data), $S = 1.03$, largest diff. peak/hole = 0.30/−0.22 e Å^{-3}, $x = 0{,}452(17)$.

3t_{Bu}: colorless crystals, $C_{25}H_{39}BN_3P$, $M_r = 423.37$, crystal size 0.22×0.08×0.06 mm, monoclinic, space group $P2_1/n$ (no.14), $a = 8.8381(6)$, $b = 14.9452(9)$, $c = 19.3839(12)$ Å, $\beta = 102.622(2)°$, $V = 2498.5$ (3) Å^3, $Z = 4$, $\rho = 1.126$ Mg m^{-1-3}, μ(Mo-K$_\alpha$) = 0.13 mm^{-1}, $F(000) = 920$, $2\theta_{max} = 55.2°$, 49835 reflections, of which 5768 were independent ($R_{int} = 0.040$), 272 parameters, $R1 = 0.045$ (for 4845 $I > 2\sigma(I)$), $wR2 = 0.113$ (all data), $S = 1.05$, largest diff. peak/ hole = 0.89/−0.38 e Å^{-3}.

3$_{Mes}$: colorless crystals, $C_{30}H_{41}BN_3P$, $M_r = 485.44$, crystal size 0.40×0.20×0.06 mm, orthorhombic, space group *Cmc*2$_1$ (no.36), $a = 16.5487(6)$, $b = 8.6092(4)$, $c = 19.6231(8)$ Å, $V = 2795.7(2)$ Å^3, $Z = 4$, $\rho = 1.153$ Mg m^{-1-3}, μ(Mo-K$_\alpha$) = 0.12 mm^{-1}, $F(000) = 1048$, $2\theta_{max} = 55.0°$, 30510 reflections, of which 3318 were independent ($R_{int} = 0.033$), 174 parameters, 1 restraint, $R1 = 0.027$ (for 3209 $I > 2\sigma(I)$), $wR2 = 0.071$ (all data), $S = 1.05$, largest diff. peak/ hole = 0.23/−0.20 e Å^{-3}, $x = 0.022(19)$.

4$_{Mes}$: colorless crystals, $C_{30}H_{41}BN_3P$, $M_r = 485.44$, crystal size 0.40×0.30×0.20 mm, monoclinic, space group $P2_1/n$ (no.14), $a = 11.2998(5)$, $b = 34.1311(14)$, $c = 14.9127(6)$ Å, $\beta = 99.415(2)°$, $V = 5674.0(4)$ Å^3, $Z = 8$, $\rho = 1.137$ Mg m^{-1-3}, μ(Mo-K$_\alpha$) = 0.12 mm^{-1}, $F(000) = 2096$, $2\theta_{max} = 55.2°$, 88690 reflections, of which 13092 were independent ($R_{int} = 0.039$), 638 parameters, $R1 = 0.048$ (for 10823 $I > 2\sigma(I)$), $wR2 = 0.114$ (all data), $S = 1.06$, largest diff. peak/ hole = 0.43/−0.34 e Å^{-3}.

5: colorless crystals, $C_{24}H_{39}BNPSi$, $M_r = 411.43$, crystal size 0.55×0.40×0.25 mm, triclinic, space group $P\bar{1}$ (no.2), $a = 9.2355(8)$, $b = 9.7839(9)$, $c = 14.8260(15)$ Å, $\alpha = 73.617(3)°$, $\beta = 73.528(3)°$, $\gamma = 76.448(3)°$, $V = 1215.1(2)$ Å^3, $Z = 2$, $\rho = 1.125$ Mg m^{-1-3}, μ(Mo-K$_\alpha$) = 0.17 mm^{-1}, $F(000) = 448$, $2\theta_{max} = 55.2°$, 23381 reflections, of which 5576 were independent ($R_{int} = 0.048$), 253 parameters, $R1 = 0.041$ (for 4947 $I > 2\sigma(I)$), $wR2 = 0.110$ (all data), $S = 1.05$, largest diff. peak/ hole = 0.44/−0.40 e Å^{-3}.

7: colorless crystals, $C_{24}H_{39}BFNPSi \cdot C_4H_{12}N$, $M_r = 504.57$, crystal size 0.20×0.08×0.03 mm, orthorhombic, *Pca*2$_1$ (no.29), $a = 17.3700(5)$, $b = 15.5606(5)$, $c = 22.4527(7)$ Å, $V = 6068.7(3)$ Å^3, $Z = 8$, $\rho = 1.105$ Mg m^{-1-3}, μ(Cu-K$_\alpha$) = 1.36 mm^{-1}, $F(000) = 2208$, $2\theta_{max} = 144.4°$, 67557 reflections, of which 10540 were independent ($R_{int} = 0.037$), 609 parameters, 212 restraints, $R1 = 0.047$ (for 10177 $I > 2\sigma(I)$), $wR2 = 0.124$ (all data), $S = 1.04$, largest diff. peak/ hole = 1.36/−0.35 e Å^{-3}, $x = 0.48(3)$.

Acknowledgements

This work was supported by the Council for Chemical Sciences of The Netherlands Organization for Scientific Research (NWO/CW) by a VIDI grant (J.C.S.) and a VENI grant (A.R.J.). We gratefully acknowledge Ed Zuidinga for mass spectrometric analyses.

Conflict of interest

The authors declare no conflict of interest.

Keywords: azides · density functional calculations · frustrated Lewis pairs · heterocycles · isocyanates

[1] a) G. D. Frey, V. Lavallo, B. Donnadieu, W. W. Schoeller, G. Bertrand, *Science* **2007**, *316*, 439 – 441; b) G. D. Frey, J. D. Masuda, B. Donnadieu, G. Bertrand, *Angew. Chem. Int. Ed.* **2010**, *49*, 9444 – 9447; *Angew. Chem.* **2010**, *122*, 9634 – 9637; c) S. Würtemberger-Pietsch, H. Schneider, T. B. Marder, U. Radius, *Chem. Eur. J.* **2016**, *22*, 13032 – 13036; d) A. F. Eichhorn, S. Fuchs, M. Flock, T. B. Marder, U. Radius, *Angew. Chem. Int. Ed.* **2017**, *56*, 10209 – 10213; *Angew. Chem.* **2017**, *129*, 10343 – 10347.

[2] For a review about recent developments on cyclic (alkyl)(amino) carbenes, see: M. Melaimi, R. Jazzar, M. Soleilhavoup, G. Bertrand, *Angew. Chem. Int. Ed.* **2017**, *56*, 10046 – 10068; *Angew. Chem.* **2017**, *129*, 10180 – 10203.

[3] For an anionic NHC, see: a) V. César, S. Labat, K. Miqueu, J.-M. Sotiropoulos, R. Brousses, N. Lugan, G. Lavigne, *Chem. Eur. J.* **2013**, *19*, 17113 – 17124; For a neutral NHC, see: b) M. Bispinghoff, A. M. Tondreau, H. Grützmacher, C. A. Faradji, P. G. Pringle, *Dalton Trans.* **2016**, *45*, 5999 – 6003.

[4] V. Lavallo, Y. Canac, B. Donnadieu, W. W. Schoeller, G. Bertrand, *Angew. Chem. Int. Ed.* **2006**, *45*, 3488 – 3491; *Angew. Chem.* **2006**, *118*, 3568 – 3571.

[5] C. Mohapatra, P. P. Samuel, B. Li, B. Niepötter, C. J. Schürmann, R. Herbst-Irmer, D. Stalke, B. Maity, D. Koley, H. W. Roesky, *Inorg. Chem.* **2016**, *55*, 1953 – 1955.

[6] For a review about organic azides, see: S. Bräse, C. Gil, K. Knepper, V. Zimmermann, *Angew. Chem. Int. Ed.* **2005**, *44*, 5188 – 5240; *Angew. Chem.* **2005**, *117*, 5320 – 5374.

[7] Recent examples of non-NHC interrupted Staudinger reactions by steric bulk: a) R. D. Kennedy, *Chem. Commun.* **2010**, *46*, 4782 – 4784; b) A. V. Alexandrova, T. Mašek, S. M. Polyakova, I. Císařová, J. Saame, I. Leito, I. M. Lyapkalo, *Eur. J. Org. Chem.* **2013**, 1811 – 1823; c) J. F. Kögel, N. C. Abacılar, F. Weber, B. Oelkers, K. Harms, B. Kovačević, J. Sundermeyer, *Chem. Eur. J.* **2014**, *20*, 5994 – 6009.

[8] For a comprehensive overview on stabilized phosphazides, see: M. W. P. Bebbington, D. Bourissou, *Coord. Chem. Rev.* **2009**, *253*, 1248 – 1261.

[9] a) H. E. Winberg, D. D. Coffman, *J. Am. Chem. Soc.* **1965**, *87*, 2776 – 2777; b) D. M. Khramov, C. W. Bielawski, *Chem. Commun.* **2005**, 4958 – 4960; c) D. J. Coady, C. W. Bielawski, *Macromolecules* **2006**, *39*, 8895 – 8897; d) D. J. Coady, D. M. Khramov, B. C. Norris, A. G. Tennyson, C. W. Bielawski, *Angew. Chem. Int. Ed.* **2009**, *48*, 5187 – 5190; *Angew. Chem.* **2009**, *121*, 5289 – 5292; e) R. S. Ghadwal, H. W. Roesky, M. Granitzka, D. Stalke, *J. Am. Chem. Soc.* **2010**, *132*, 10018 – 10020; f) A. A. Grishina, S. M. Polyakova, R. A. Kunetskiy, I. Císařová, I. M. Lyapkalo, *Chem. Eur. J.* **2011**, *17*, 96 – 100; g) D. Jishkariani, C. D. Hall, A. Demircan, B. J. Tomlin, P. J. Steel, A. R. Katritzky, *J. Org. Chem.* **2013**, *78*, 3349 – 3354; h) F. W. Kimani, J. C. Jewett, *Angew. Chem. Int. Ed.* **2015**, *54*, 4051 – 4054; *Angew. Chem.* **2015**, *127*, 4123 – 4126.

[10] For a recent review on π-conjugated triazenes, see: S. Patil, A. Bugarin, *Eur. J. Org. Chem.* **2016**, 860 – 870.

[11] a) D. M. Khramov, C. W. Bielawski, *J. Org. Chem.* **2007**, *72*, 9407 – 9417; b) S. Patil, K. White, A. Bugarin, *Tetrahedron Lett.* **2014**, *55*, 4826 – 4829.

[12] a) J. M. Hopkins, M. Bowdridge, K. N. Robertson, T. S. Cameron, H. A. Jenkins, J. A. C. Clyburne, *J. Org. Chem.* **2001**, *66*, 5713 – 5716; b) M. Tamm, S. Randoll, T. Bannenberg, E. Herdtweck, *Chem. Commun.* **2004**, 876 – 877; c) M. Tamm, D. Petrovic, S. Randoll, S. Beer, T. Bannenberg, P. G. Jonesa, J. Grunenberg, *Org. Biomol. Chem.* **2007**, *5*, 523 – 530; d) S. Lysenko, C. G. Daniliuc, P. G. Jones, M. Tamm, *J. Organomet. Chem.* **2013**, *744*, 7 – 14.

[13] a) D. W. Stephan, G. Erker, *Angew. Chem. Int. Ed.* **2010**, *49*, 46 – 76; *Angew. Chem.* **2010**, *122*, 50 – 81; b) D. W. Stephan, *Acc. Chem. Res.* **2015**, *48*, 306 – 316; c) D. W. Stephan, *Science* **2016**, *354*, aaf7229; d) A. R. Jupp, D. W. Stephan, *New Trends Chem. Teach. Trends Chem.* **2019**, *1*, 35 – 48.

[14] a) C. M. Mömming, G. Kehr, B. Wibbeling, R. Fröhlich, G. Erker, *Dalton Trans.* **2010**, *39*, 7556 – 7564; b) A. Stute, L. Heletta, R. Fröhlich, C. G. Daniliuc, G. Kehr, G. Erker, *Chem. Commun.* **2012**, *48*, 11739 – 11741; c) X. Xu, G. Kehr, C. G. Daniliuc, G. Erker, *J. Am. Chem. Soc.* **2013**, *135*, 6465 – 6476; d) J. Schneider, K. M. Krebs, S. Freitag, K. Eichele, H. Schubert, L. Wesemann, *Chem. Eur. J.* **2016**, *22*, 9812 – 9826; e) L. Keweloh, H. Klöcker, E.-U. Würthwein, W. Uhl, *Angew. Chem. Int. Ed.* **2016**, *55*, 3212 – 3215; *Angew. Chem.* **2016**, *128*, 3266 – 3269; f) L.-M. Elmer, G. Kehr, C. G. Daniliuc, M. Siedow, H. Eckert, M. Tesch, A. Studer, K. Williams, T. H. Warren, G. Erker, *Chem. Eur. J.* **2017**, *23*, 6056 – 6606; g) J. Backs, M. Lange, J. Possart, A. Wollschläger, C. Mück-Lichtenfeld, W. Uhl, *Angew. Chem. Int. Ed.* **2017**, *56*, 3094 – 3097; *Angew. Chem.* **2017**, *129*, 3140 – 3143.

[15] M. W. P. Bebbington, S. Bontemps, G. Bouhadir, D. Bourissou, *Angew. Chem. Int. Ed.* **2007**, *46*, 3333 – 3336; *Angew. Chem.* **2007**, *119*, 3397 – 3400.

[16] A. Stute, G. Kehr, R. Fröhlich, G. Erker, *Chem. Commun.* **2011**, *47*, 4288 – 4290.

[17] Two examples are reported for addition of an intermolecular FLP to the α- and γ-nitrogen of an azide, see: a) J. Zhou, L. L. Cao, L. L. Liu, D. W. Stephan, *Dalton Trans.* **2017**, *46*, 9334 – 9338; b) T. C. Johnstone, G. N. J. H. Wee, D. W. Stephan, *Angew. Chem. Int. Ed.* **2018**, *57*, 5881 – 5884; *Angew. Chem.* **2018**, *130*, 5983 – 5986.

[18] D. Pleschka, M. Layh, F. Rogel, W. Uhl, *Philos. Trans. R. Soc. London Ser. A* **2017**, *375*, 20170011.

[19] a) F. Bertini, V. Lyaskovskyy, B. J. J. Timmer, F. J. J. de Kanter, M. Lutz, A. W. Ehlers, J. C. Slootweg, K. Lammertsma, *J. Am. Chem. Soc.* **2012**, *134*, 201 – 204; b) E. R. M. Habraken, L. C. Mens, M. Nieger, M. Lutz, A. W. Ehlers, J. C. Slootweg, *Dalton Trans.* **2017**, *46*, 12284 – 12292; c) D. H. A. Boom, A. W. Ehlers, M. Nieger, J. C. Slootweg, *Z. Naturforsch. B: Chem. Sci.* **2017**, *72*, 781 – 784.

[20] Compound $\mathbf{2_{Ph}}$, $\mathbf{3_{tBu}}$, $\mathbf{3_{Mes}}$, and $\mathbf{4_{Mes}}$ showed decomposition when solutions were handled in the presence of light and therefore all reactions were performed in the absence of light.

[21] For computational studies on the Staudinger reaction, see: a) M. Alajarin, C. Conesa, H. S. Rzepa, *J. Chem. Soc. Perkin Trans. 2* **1999**, 1811 – 1814; b) W. Q. Tian, Y. A. Wang, *J. Org. Chem.* **2004**, *69*, 4299 – 4308; c) W. Q. Tian, Y. A. Wang, *J. Chem. Theory Comput.* **2005**, *1*, 353 – 362.

[22] For a review on the coordination chemistry of organic azides, see: S. Cenini, E. Gallo, A. Caselli, F. Ragaini, S. Fantauzzi, C. Piangiolino, *Coord. Chem. Rev.* **2006**, *250*, 1234 – 1253.

[23] DFT supported intermediates and isolated complexes of organic azides with cobalt: a) V. Lyaskovskyy, A. I. O. Suarez, H. Lu, H. Jiang, X. P. Zhang, B. de Bruin, *J. Am. Chem. Soc.* **2011**, *133*, 12264 – 12273; ruthenium: b) P. Zardi, A. Pozzoli, F. Ferretti, G. Manca, C. Meallic, E. Gallo, *Dalton Trans.* **2015**, *44*, 10479 – 10489; rhodium: c) S. H. Park, J. Kwak, K. Shin, J. Ryu, Y. Park, S. Chang, *J. Am. Chem. Soc.* **2014**, *136*, 2492 – 2502; iron: d) J. Li, C. Wu, Q. Zhanga, B. Yan, *Dalton Trans.* **2013**, *42*, 14369 – 14373; gold: e) C. Dash, M. Yousufuddin, T. R. Cundari, H. V. R. Dias, *J. Am. Chem. Soc.* **2013**, *135*, 15479 – 15488; iridium: f) G. Albertin, S. Antoniutti, D. Baldan, J. Castro, S. García-Fontán, *Inorg. Chem.* **2008**, *47*, 742 – 748; silver: g) H. V. R. Dias, S. A. Polach, S.-K. Goh, E. F. Archibong, D. S. Marynick, *Inorg. Chem.* **2000**, *39*, 3894 – 3901.

[24] a) J. S. Thayer, R. West, *Inorg. Chem.* **1965**, *4*, 114 – 115; b) J. Kouvetakis, J. McMurran, P. Matsunaga, M. O'Keeffe, J. L. Hubbard, *Inorg. Chem.* **1997**, *36*, 1792 – 1797; c) K. Bläsing, J. Bresien, R. Labbow, D. Michalik, A. Schulz, M. Thomas, A. Villinger, *Angew. Chem. Int. Ed.* **2019**, *58*, 6540 – 6544; *Angew. Chem.* **2019**, *131*, 6610 – 6615.

[25] A broad $^{31}P\{^{1}H\}$ NMR signal was observed for $\mathbf{3_{Mes}}$ at room temperature ($\nu_{1/2} \approx 235$ Hz), which upon cooling to 223 K split into two signals at $\delta =$ +98.6 and +89.4 ppm in a 93:7 ratio. The structure of these isomers is still to be determined. For comparison, see Ref. [12a].

[26] Note that the geometry of the phenyl analogue of **INT2** ($\mathbf{INT2_{Ph}}$) could not be optimized without constraints. For more information see the supporting information.

[27] The computational details for all mechanisms with Ph–N_3, *t*Bu–N_3, Mes–N_3, and TMS–N_3 can be found in the Supporting Information.

[28] See the Supporting Information.

[29] O. Alhomaidan, E. Hollink, D. W. Stephan, *Organometallics* **2007**, *26*, 3041 – 3048.

[30] P. Paetzold, R. Truppat, *Chem. Ber.* **1983**, *116*, 1531 – 1539.

[31] A similar mechanism to was proposed earlier by Brown and co-workers in which the migration of a boron-substituent was proposed during the dinitrogen elimination, see: a) H. C. Brown, A. Suzuki, S. Sonao, M. Itoh, M. M. Midland, *J. Am. Chem. Soc.* **1971**, *93*, 4329 – 4330; b) H. C. Brown, M. M. Midland, A. B. Levy, H. C. Brown, R. B. Wetherill, A. Suzuki, S. Sono, M. Itoh, *Tetrahedron* **1987**, *43*, 4079 – 4088.

[32] a) S. Roters, C. Appelt, H. Westenberg, A. Hepp, J. C. Slootweg, K. Lammertsma, W. Uhl, *Dalton Trans.* **2012**, *41*, 9033 – 9045; b) F. Bertini, F. Hoffmann, C. Appelt, W. Uhl, A. W. Ehlers, J. C. Slootweg, K. Lammertsma, *Organometallics* **2013**, *32*, 6764 – 6769.
[33] P. Spies, G. Erker, G. Kehr, K. Bergander, R. Fröhlich, S. Grimme, D. W. Stephan, *Chem. Commun.* **2007**, 5072 – 5074.
[34] For examples of P=N–Si motifs with a large bond angle, see: a) A. Armstrong, T. Chivers, M. Krahn, M. Parvez, G. Schatte, *Chem. Commun.* **2002**, 2332 – 2333; b) E. Hollink, J. C. Stewart, P. Wei, D. W. Stephan, *Dalton Trans.* **2003**, 3968 – 3974; c) T. W. Graham, J. Kickham, S. Courtenay, P. Wei, D. W. Stephan, *Organometallics* **2004**, *23*, 3309 – 3318.
[35] a) S. Moebs-Sanchez, G. Bouhadir, N. Saffon, L. Maron, D. Bourissou, *Chem. Commun.* **2008**, 3435 – 3437; b) K. V. Axenov, C. M. Mömming, G. Kehr, R. Fröhlich, G. Erker, *Chem. Eur. J.* **2010**, *16*, 14069 – 14073; c) W. Uhl, J. Possart, A. Hepp, M. Layh, *Z. Anorg. Allg. Chem.* **2017**, *643*, 1016 – 1029.
[36] Only one other example of an iminophosphorane Lewis base in FLP chemistry is reported, see: C. Jiang, D. W. Stephan, *Dalton Trans.* **2013**, *42*, 630 – 637.
[37] H. A. Duong, M. J. Cross, J. Louie, *Org. Lett.* **2004**, *6*, 4679 – 4681.
[38] Y. Taguchi, I. Shibuya, M. Yasumoto, T. Tsuchiya, K. Yonemoto, *Bull. Chem. Soc. Jpn.* **1990**, *63*, 3486 – 3489.
[39] S. M. Raders, J. G. Verkade, *J. Org. Chem.* **2010**, *75*, 5308 – 5311.
[40] Z. Pusztai, G. Vlad, A. Bodor, I. T. Horváth, H. J. Laas, R. Halpaap, F. U. Richter, *Angew. Chem. Int. Ed.* **2006**, *45*, 107 – 110; *Angew. Chem.* **2006**, *118*, 113 – 116.
[41] D. Heift, Z. Benkő, H. Grützmacher, A. R. Jupp, J. M. Goicoechea, *Chem. Sci.* **2015**, *6*, 4017 – 4024.
[42] J. C. Bottaro, P. E. Penwell, R. J. Schmitt, *Synth. Commun.* **1997**, *27*, 1465 – 1467.
[43] C. Zanato, M. G. Cascio, P. Lazzari, R. Pertwee, A. Testa, M. Zanda, *Synthesis* **2015**, *47*, 817 – 826.
[44] D. G. Brown, N. Sanguantrakun, B. Schulze, U. S. Schubert, C. P. Berlinguette, *J. Am. Chem. Soc.* **2012**, *134*, 12354 – 12357.
[45] A. A. Kolomeitsev, F. U. Seifert, G.-V. Röschenthaler, *J. Fluorine Chem.* **1995**, *71*, 47 – 49.
[46] G. M. Sheldrick, *Acta Crystallogr. Sect. A* **2008**, *64*, 112 – 122.
[47] G. M. Sheldrick, *Acta Crystallogr. Sect. A* **2015**, *71*, 3 – 8.
[48] G. M. Sheldrick, *Acta Crystallogr. Sect. C* **2015**, *71*, 3 – 8.
[49] S. Parsons, H. D. Flack, T. Wagner, *Acta Crystallogr. Sect. B* **2013**, *69*, 249 – 259.
[50] CCDC 1896718, 1896719, 1896720, 1896721, 1896722, and 1896723 contain the supplementary crystallographic data for this paper. These data are provided free of charge by The Cambridge Crystallographic Data Centre.

Manuscript received: June 12, 2019
Version of record online: ■■ ■■, 0000

FULL PAPER

One plus one equals 4, 5, or 6: The geminal frustrated Lewis pair tBu$_2$PCH$_2$BPh$_2$ reacts with phenyl-, mesityl-, *tert*-butyl and trimethylsilyl azide affording, respectively, six, five, and four-membered rings as isolable products. DFT calculations revealed that the formation of all products proceeds via the six-membered ring structure, which is the thermodynamic product with an *N*-phenyl group, but rearranges when sterically more encumbered substituents are used.

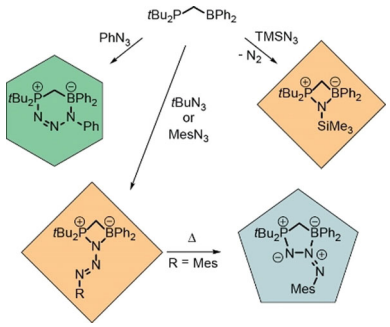

Frustrated Lewis Pairs

*D. H. A. Boom, A. R. Jupp, M. Nieger, A. W. Ehlers, J. C. Slootweg**

■■ – ■■

New Insights in Frustrated Lewis Pair Chemistry with Azides

An intramolecular frustrated Lewis pair has been shown to react with different organic azides to form a range of 4, 5 and 6-membered heterocycles, and the varying reaction paths are rationalized computationally. The product derived from trimethylsilyl azide rapidly extrudes nitrogen, and the resulting cyclized iminophosphorane/borane adduct was explored as a catalyst for the trimerization of isocyanates. For more information, see the Full Paper by C. Slootweg et al. on page ■ ■ ff.